The Implementation of Polystyrene and Graphene in the Active Layer of PCDTBT:PCBM Inverted Organic Solar Cells to Increase Energy Conversion Efficiency

Andrew Wang [1,§], Effie Jia [2,§], Zhen-Hua Yang [3,†], Crisleine Saleri [3,†], and Miriam Rafailovich [3,†]
[1] Nikola Tesla STEM High School, Redmond, Washington 98074
[2] Dougherty Valley High School, San Ramon, California 94582
[3] Department of Materials Science, Stony Brook University, Stony Brook, New York 11794

The Implementation of Polystyrene and Graphene in the Active Layer of PCDTBT:PCBM Inverted Organic Solar Cells to Increase Energy Conversion Efficiency

Abstract

Rising energy demand and concern over the effect of fossil fuels on global climate change have increased interest in renewable energy technology. Photovoltaics (PV) offer passive energy generation and versatility due to the different types of PV systems available from flexible organic thin film systems to more rigid inorganic systems. Organic solar cells optimized for higher Power Conversion Efficiency (PCE) through the implementation of Polystyrene and Graphene in the polymer active layer are one type of engineered PV solutions.

The engineered PV cells were compared primarily through their PCE. The first parameter tested was the effect of thin film spin speed on PCE, where data collected indicated that a speed of 3000 rpm and thus a thinner film (confirmed via SEM) resulted in a higher PCE of 1.915%. The following tested parameter was the effect of PS on PCE, where data collected indicated that a concentration of 2 mg/mL of PS corresponded to a peak PCE of 2.365%. The final parameter tested was the effect of Graphene on PCE, where data collected indicated that the addition of graphene increased PCE to 2.523%. Collectively, the changes studied resulted in an overall increase in efficiency of 31.72%.

1. Introduction

In recent years, climate change has taken center stage as the driving factor for pushing market growth. Increasingly negative sentiments towards exhaustible resource based energy production, such as fossil fuels, have given the renewable energy industry new light. Solar energy is one of the most promising fields of the renewable energy sector to become the primary source of energy production worldwide. In the past five years, the total installed capacity worldwide has nearly doubled and has been growing at an exponential rate since the year 2000[19]. Early research primarily centered on the development of rigid non-organic solar cells due to their high power conversion efficiency. However, current research is leading towards organic solar cells for their high versatility in use despite their low efficiencies.

Organic Solar Cells

Organic solar cells, or plastic solar cells, are a polymer based PV system that utilize photosensitive organic polymers for light absorption and charge transfer to generate energy via the photovoltaic effect. Organic solar cells are typically structured in one of two ways: standard or inverted[20]. The standard structure utilizes electron transport and hole blocking to generate electricity while the inverted structure does the opposite[9]. Organic solar cells show promise for widespread commercial application due to its low weight, flexibility, disposability, inexpensive production, and versatile applicability due to its thin film structure. However, organic solar cells also see significant shortcomings as a result of their beneficial properties. These PV systems only offer one-third of the power conversion efficiency of non-organic solar cells and also experience substantial photochemical degradation.

Active Layer Morphology

The Planar Heterojunction (PHJ) structure for solar cells is the simplest active layer structure utilized in organic polymer solar cells. In the PHJ structure, a film of active polymer (donor) and a polymer film of electron accepting material (acceptor) is spun cast between contacts. Excitons created in the donor material can then pass to the junction and split, sending the hole back to the donor and the electron to the acceptor. However, charge carriers typically have

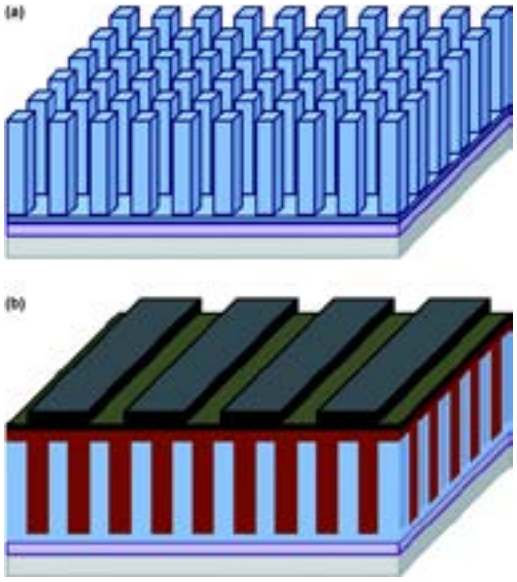

Figure 1: The ideal active layer morphology of an organic solar cell[1]

junctions ranging from 3-10 nanometers and as a result, organic polymer solar cells must be thin and thus absorb light less efficiently[18].

The Bulk Heterojunction (BHJ) structure for solar cells aims to increase efficiency through a blend of donor and acceptor materials with phase separations, as seen in Figure 1. In fact, regions of each material are typically several nanometers apart, making the interface suitable for carrier diffusion[14]. However, because there is no uniform structure between the different phases, BHJ cells have high variability due to a greater risk of recombination between the electron and hole[6]. As such, optimizing the efficiency of a BHJ cell requires precise control of the morphology of the materials in the active layer[2].

Ordered Heterojunction (OHJ) structures solve the variability of BHJs while maintaining the ideal phase separation distance. OHJ structures are typically hybrid combinations of organic active materials and inorganic ordered materials. Therefore, it is important for the organic and inorganic materials to be immiscible in a spun cast thin film. Typical inorganic ordered materials are plastic polymers since they are generally immiscible with commonly used active materials.

The goal of this experiment is to achieve the OHJ structure and create a columnar morphology in order to reduce the risk of recombination, and thus, increase conversion efficiency. The implementation of polystyrene in the active layer is predicted to create the ideal structure, while the addition of graphene is predicted to increase efficiency due to its conductive characteristics. The ultimate desired result is to see an overall increase in power conversion efficiency (PCE) of organic solar cells.

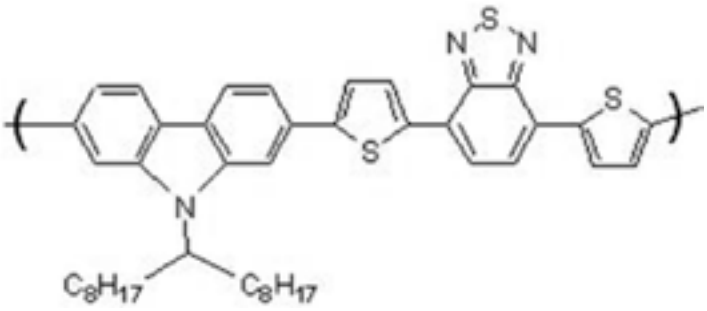

Figure 2: Chemical structure of PCDTBT[16]

PCDTBT

PCDTBT (Figure 2) is widely regarded as a part of the next generation of electron donor materials for organic photovoltaic (OPV) systems[3]. The primary characteristic of PCDTBT that raises interest in its application in OPV systems is the material's low highest occupied molecular orbital (HOMO) and lowest unoccupied molecular orbital (LUMO). These molecular properties result in increased open circuit voltage (VOC), longer wavelength absorption, and improved stability in ambient conditions. Furthermore, PCDTBT is highly soluble in Chlorobenzene (CB), a common solvent for PCBM and Polystyrene.

PCBM

PCBM (Figure 3), or Phenyl-C61-butyric acid methyl ester, is a fullerene derivative of a C60 buckyball. Often used as an electron acceptor in

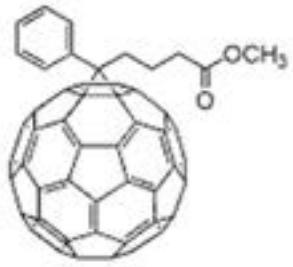

Figure 3: PCBM[15]

organic polymer solar cells, PCBM is the most practical choice for an electron accepting material due to its high solubility in Chlorobenzene (CB), a widely used solvent for organic PV systems[19]. In fact, its solubility offers potential for innovative technology development such as printable PV systems. However, its high production cost due to the process of fabricating fullerenes is a limit for its commercial scale applicability.

Polystyrene

Polystyrene (Figure 4) is a synthetic aromatic polymer consisting of a long chain of the styrene

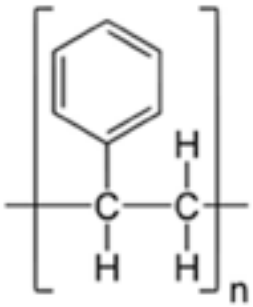

Figure 4: Polystyrene[17]

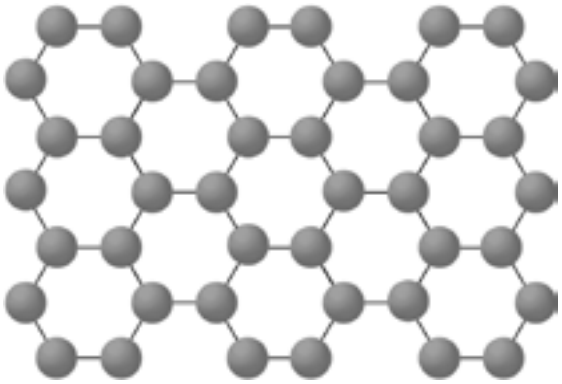

Figure 5: Graphene[4]

monomer. Polystyrene is one of the most commonly utilized plastics, with its production reaching up to several billion kilograms per year. Furthermore, polystyrene has a low melting point and high solubility in Chlorobenzene, making it a commonly used morphological control agent for OPV system research[12]. In addition, the hydrophobicity of polystyrene further exhibits its applicability as a phase separating material.

Graphene

Graphene is an allotrope of carbon in the form of a two-dimensional honeycomb lattice at the atomic level where each vertex consists of a carbon atom in a single atom thick sheet. Since its discovery in 2010 by Andre Geim and Konstantin Novoselov, graphene has captivated scientists with its incredible properties. Chemically, graphene's sp^2 orbital hybridization is largely responsible for its unparalleled thermal and electrical conductivity. Physically, graphene is 200 times stronger than steel and transparent. Collectively, these properties make graphene an excellent addition to the active layer of an OPV cell[10]. Graphene provides rigid highly conductive low-resistance pathways for the facilitation of exciton dissociation and carrier transportation within the active layer.

2. Methods

The initial samples produced in the standard organic cell structure. For device fabrication, indium tin oxide (ITO)-coated glass slides were polished in UV ozone for 10 minutes. A 50 nm thick poly(3,4-ethylenedioxythiophene)-poly(styrenesulfonate) (PEDOT:PSS) layer was spun-cast onto the ITO glass at 5000 rpm for 45 seconds and was baked at 140 °C for 10 minutes on the hot plate exposed to the air[11]. Chlorobenzene (CB) solutions composed of 16 mg/mL of PCDTBT and PCBM in weight ratio 4:12 and 18 mg/mL of PCDTBT,

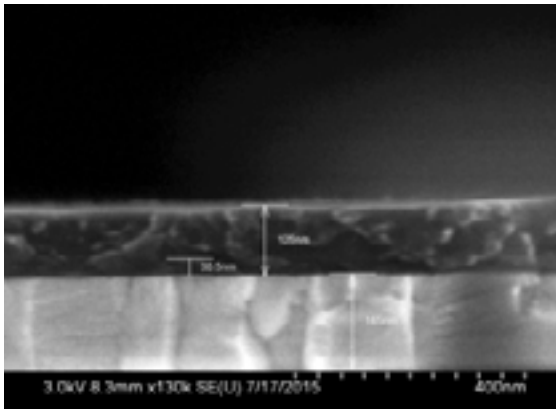

Figure 6: SEM image of PCDTBT:PS:PCBM (4:2:12) produced in the standard OPV structure

---

polystyrene, and PCBM of weight ratio 4:2:12 (Figure 6) were spun-cast onto the previously deposited PEDOT:PSS layer separately at 2000 rpm for 45 seconds. Both samples were spun-cast in air. Aluminum electrodes with 100 nm thickness were then deposited onto the sample at 1 Å/s speed in physical vapor deposition (PVD) at a pressure lower than 3 × 10−7 Pa. The whole device was then annealed in a vacuum oven at 150 °C for one hour.

Following samples were produced utilizing an inverted organic cell structure. For device fabrication, indium tin oxide (ITO)-coated glass slides were polished in UV-ozone for 10 minutes. A TiO_2 solution was synthesized according to Xue et. al. A 30 nm thick TiO_2 layer was spun-cast onto the ITO glass at 3000 rpm for 20 seconds and was baked at 400 °C for 2 hours on a hot plate exposed to air[21]. Chlorobenzene (CB) solutions composed of PCDTBT, polystyrene, and PCBM in weight ratios 4:0:12, 4:2:12, and 4:2:8 mg/mL were spun-cast at 3000 rpm for 45 seconds on top of the TiO_2 layer in air[22]. The typical thickness of the active layer was found to be around 80 nm. Device samples were then annealed in a vacuum oven at 150 °C for 10 minutes. Finally, the devices were complete by thermal evaporation of 8 nm MoO_3 and a 100 nm Ag electrode with the help of Kurt J. Lesker PVD 75 vacuum deposition systems.

Devices were then fabricated utilizing graphene as an additive to the active layer solution. Before fabrication, 3 nm Graphene Nanopowder (Graphene Supermarket) was dissolved in chlorobenzene. A 1.0 mg/mL solution of graphene was produced and sonicated for ten hours. Afterwards, the solution was centrifuged at 3600 rpm for one hour and repeatedly done so until there was no visible sign of graphene solute present[7]. The supernatant fluid was then deposited onto a cleaned glass slide and let dry. The sample was then tested

for graphene utilizing UV-Vis spectroscopy, atomic force microscopy, and analyzed under an optical microscope. Through these procedures, it was observed that certain amounts of dissolved graphene were present in the sample While results were inconclusive regarding the precise amount of graphene, it was determined that graphene's solubility in chlorobenzene was adequate for the parameters being tested in this procedure.

With the solubility of graphene found adequate for device fabrication, 0.6 mL solutions were produced of weight ratio 4:2:12:0.1, 4:2:12:0.15, and 4:2:8:0.1 mg/mL of PCDTBT, polystyrene, PCBM, and graphene. The devices were then fabricated according to the process described above for the inverted organic cell structure.

The performance of the solar cell devices were tested by a 150 W solar simulator (Oriel) with an AM 1.5G filter for solar illumination. The light intensity was calibrated to 100 mW cm−2 by a calibrated thermopile detector (Oriel). Data was collected according to procedures described by Pan et. al.

Additional samples were fabricated for alternative data collection. 0.6 mL solutions of weight ratios 4:0:12:0, 4:2:12:0, 4:0:4:0, and 4:2:12:0.1 mg/mL of PCDTBT, polystyrene, PCBM, and graphene were produced. The solutions were spun cast on cleaned glass substrates at 3000 rpm for 45 seconds[8]. After UV-Vis absorption and atomic force microscope data were collected, a 4:0:4:0 sample and a 4:2:12:0 sample were washed with cyclohexane and acetone, respectively, to selectively dissolve polystyrene and the samples were then retested using the atomic force microscope.

Atomic Force Microscopy (AFM) data was collected utilizing a Digital Instruments atomic force microscope. All AFM data was collected using a 10 μm by 10 μm scan area and the contact AFM methodology. Device samples and samples prepared for alternative data collection were both utilized in the AFM. Furthermore, samples were tested using the current AFM methodology in a Bruker Dimension Icon AFM set to test current via high frequency tapping and 5V stimulation. However, long scan times resulted in a high incidence of error, resulting in unusable data.

UV-Vis absorption data was collected utilizing a Thermo Scientific Evolution™ 220 UV-Visible Spectrophotometer. All UV-Vis

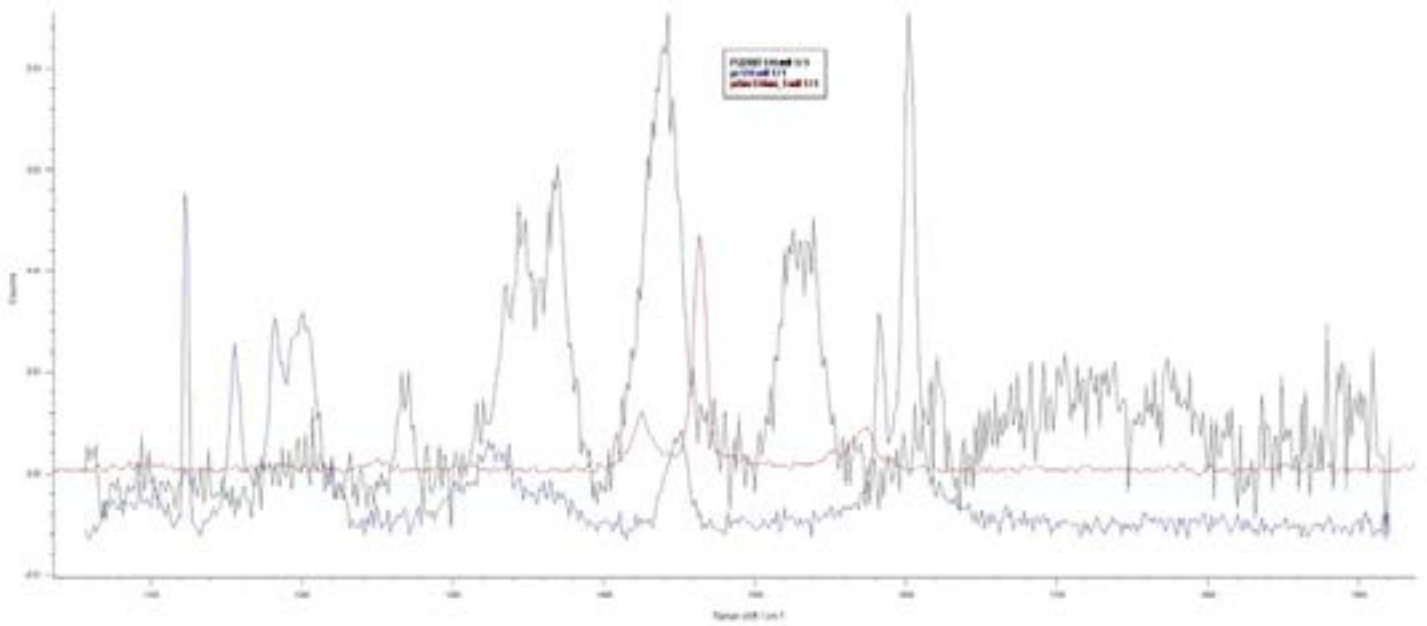

Figure 7: Collected Raman spectrum of PCDTBT (black), PS (blue), and PCBM (red)

data was collected using a scan with a starting wavelength of 800 nm and ending wavelength of 300 nm. Samples prepared for alternative data collection were analyzed in the UV-Vis spectrophotometer. However, the spectrophotometer was manufactured for use in testing the absorption of liquids in a cuvette. As such, samples were taped into place using clear scotch tape for data collection.

Raman-SPM/AFM data (Figure 7) was collected with a Renishaw inVia confocal Raman microscope coupled with a Bruker Dimension Icon AFM. Raman-SPM/AFM data was collected using a scan area of 10 µm by 10 µm, a laser power of 1%, and two one second accumulations centered at 1650. Raman data was then utilized to determine the separation of phases within the tested sample.

3. Results and Discussion

Devices were analyzed quantitatively through efficiency data collected using solar simulation. The thin film active layer was analyzed qualitatively through morphology data collected utilizing various equipment. Qualitative data collection was completed using both device samples and samples produced for spe-

cific collection methods. The main methods of analyzation used were AFM, Raman-SPM, and solar simulation.

Implementation of Polystyrene and Graphene

When Polystyrene (PS) was incorporated into the devices, AFM and Raman-SPM data indicated that the addition of the polymer resulted in a columnar structure, creating a uniform phase-separation of PCDTBT and PCBM. This was proven through the use of selective solvents and the subsequent dissolution of PS. First, a thin film consisting of PCDTBT and PS was spin-cast and then annealed for 10 minutes. Afterwards, the film was placed into cyclohexane in order to dissolve the PS. Cyclohexane was chosen as the solvent because it was predicted to dissolve most of the PS without dissolving much of the PCDTBT. This was successful, and it was determined that the PS had created a columnar structure because "island structures" were visible where PS had been previously located as seen in Figures 8 and 9. The areas in Figure 9 that are darker indicate lower sections of the film, demonstrating the lack of PS. These findings were further confirmed via Transmission Electron Microscopy images in Figure 10, where phase-separation is evident.

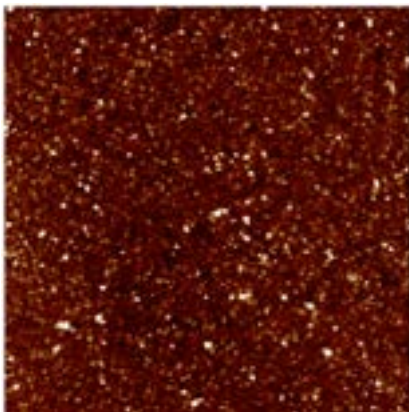

Figure 8: PCDTBT:PS:PCBM (4:2:12) annealed for 10 minutes

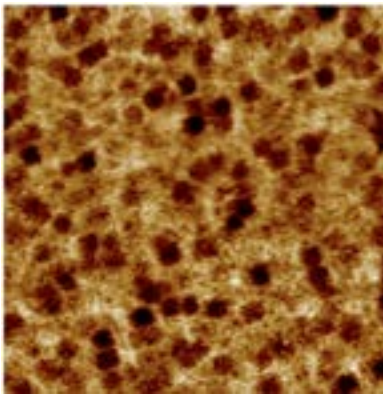

Figure 9: PCDTBT:PS:PCBM (4:2:12) annealed for 10 minutes and washed with cyclohexane

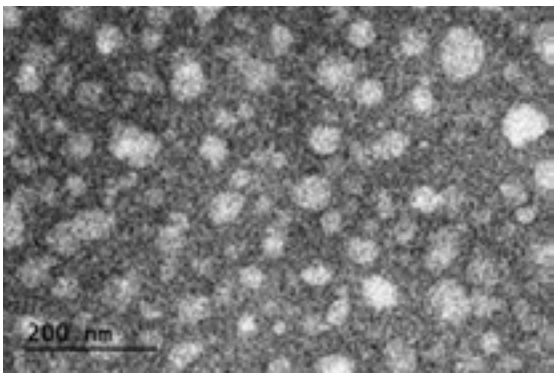

Figure 10: TEM image of a device sample with active layer ratio 4:2:12:0

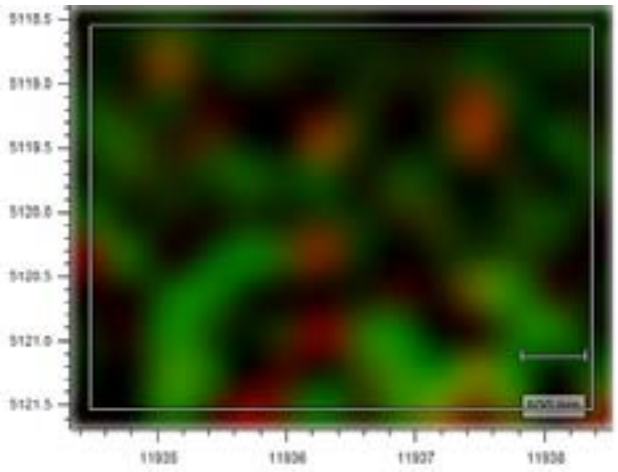

Figure 11: Raman-SPM/AFM
Green = PCDTBT Red = PS

Looking at the contrasting high and low areas of Figures 8 and 9, it was crucial to determine that columnar structure was achieved by the addition of PS. This confirmed the prediction that the implementation of the polymer would result in a greater PCE due to a shortened travel distance of the electron and its hole. Consequently, there would be a lower risk of electron-hole recombination, further improving conversion efficiency.

The Raman spectrum that was produced (Figure 7) also demonstrates the phase-separation of the active layer materials. The spectrum differs for each polymer, indicating that there is a clear separation between each material. PCDTBT, PS, and PCBM can all be distinguished from each other in the spectrum, having distinct peaks at about 1440, 1460, and 1470 Raman shift/cm^{-1}.

Through Conductive AFM of the active layer, regions of PCBM were identified and observed to be circularly surrounding sections of PS. Thus, it was determined that the presence of PS resulted in a phase-separation of the donor and acceptor materials due to PCBM's tendency to circumscribe columns of PS. Furthermore, Conductive AFM demonstrated that PCBM was a strong conductive material, carrying the electrical current through the active layer.

The Raman-SPM/AFM image shown in Figure 11 greatly demonstrates that there was a distinct phase-separation between the active layer materials. The green indicates the presence of PCDTBT while the red indicates that of PS. It clearly shows that a uniform structure was achieved through the addition of PS, confirming that the properties of polystyrene led to the ideal OHJ structure. Furthermore, it allowed for the identification of polymers, unlike the AFM images. From the simultaneous use of Raman-SPM and AFM, it was able to determine which areas were composed of PCDTBT and which ones con-

Average Contact Angle for Devices Containing Polystyrene

Active Layer Ratio*	4:0.5:12:0	4:2:12:0	4:2:12:0 2000 RPM	4:2:12:0 3000 RPM	4:2:12:0 10 min Anneal	4:2:12:0.1 3000 RPM
Average Contact Angle (°)	1.329	2.239	2.412	1.456	2.996	1.889

*Active Layer Ratio refers to the ratio of PCDTBT:PS:PCBM:Graphene

Table 1: Average contact angle

tained PS. This data greatly helped not only to confirm the predicted phase-separation, but also to differentiate each polymer.

Device samples containing PS were additionally evaluated based on average contact angle through the use of Nanoscope™. Utilizing AFM images collected, data in Table 1 shows a rise in contact angle, and thus hydrophobicity, as the ratio of PS increases. In addition, device fabrication at higher spin speeds correlated with decreases in contact angle while device fabrication with a longer annealing duration correlated with an increase in contact angle[13]. Furthermore, the addition of graphene corresponded with an increase to hydrophobicity, as seen through the higher average contact angle of 1.889.

UV-Vis data shown in Figure 12 indicates significant peaks in absorption outside of the visible light spectrum. The addition of polystyrene to the active layer decreased light absorption along the spectrum range of around 270 nm to 800 nm. However, the addition of both graphene and polystyrene to the active layer resulted in an increase in light absorption along the same range when compared to the standard sample. This increase in absorption contributed to the increase in conversion efficiency since the cells were able to take in a greater range of light. Since different materials have different absorption spectrums, the UV-Vis data confirmed the presence of each polymer and their spectras.

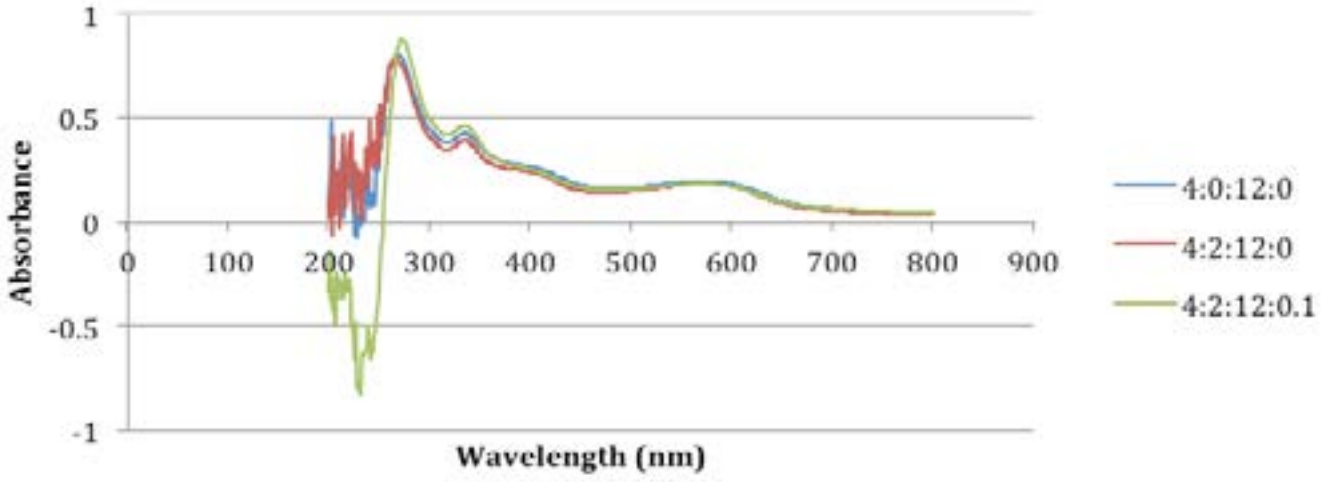

Figure 12: UV-Vis absorption spectrum for various devices

Device Efficiency

Under simulated solar light irradiation with intensity of 100 mW cm−2, the photovoltaic parameters of the inverted solar cell including short circuit current density (J_{SC}), open circuit voltage (V_{OC}), fill factor (FF), and energy conversion efficiency (η) were measured and are given in Table 2. Solar simulation was done to test the conversion efficiency of the cells.

As shown in Table 2, the implementation of polystyrene to the 4:0:12:0 device resulted in increases across the board in short circuit current density (J_{SC}), open circuit voltage (V_{OC}), fill factor (FF), and energy conver-

Average Device Efficiency

Active Layer Ratio*	J_{SC} (mA/cm^2)	V_{OC} (V)	FF	η (%)
4:0:12:0	5.66	0.695	0.487	1.92
4:2:12:0	6.00	0.795	0.497	2.37
4:2:8:0	4.10	0.763	0.445	1.45
4:2:12:0.1	6.65	0.760	0.498	2.52
4:2:8:0.1	3.96	0.768	0.482	1.47
4:2:12:0.15	5.59	0.733	0.432	1.77

*Active Layer Ratio refers to the ratio of PCDTBT:PS:PCBM:Graphene

Table 2: Average device efficiency of organic solar cells

sion efficiency (η) due to the columnar structure and phase separation exhibited in previous images. Furthermore, the addition of graphene to the 4:2:12:0, while decreasing open circuit voltage (V_{OC}) also increased short circuit current (J_{SC}) thus correlating to a significant increase in energy conversion efficiency (η). Table 2 shows that the addition of graphene led to the highest average device efficiency of 2.52%

Devices with lower concentrations of PCBM were tested to determine if the increase in energy conversion efficiency was inhibited by the amount of PCBM within the concentration. The devices with reduced PCBM, 4:2:8:0 and 4:2:8:0.1, both showed lower energy conversion efficiencies (η) and exhibited decreased efficacy of graphene in the active layer. Devices with higher concentrations of graphene were tested to determine the relationship between the amount graphene within the solution and its effect on energy conversion efficiency (η). The 4:2:12:0.15 device exhibited results indicating that the addition of excess graphene to the active layer solution resulted in a significantly reduced fill factor (FF) and therefore a significant decrease in the energy conversion efficiency (η) when compared to the standard. Under the ideal testing conditions of the parameters manipulated in this experiment, the device of active layer ratio 4:2:12:0.1 displayed an energy conversion efficiency (η) of 2.52%, a 31.72% increase in efficiency in comparison to the standard device ratio 4:0:12:0 that displayed an energy conversion efficiency of 1.92%. This suggests that the ratio of PCBM:Graphene was most effective at the 12:0.1 level. In terms of J_{SC}, V_{OC}, FF, and η, the 4:2:12:0.1 device generally performed the best in all the parameters.

4. Conclusion

The organic photovoltaic active layer solutions present in this study indicate that the addition of polystyrene to PCDTBT and PCBM solutions achieves columnar structures where PCBM primarily aggregates at the interfaces. The two phases are created due to the phase separation that occurs between polystyrene and PCDTBT, which has been confirmed by Raman-SPM, AFM, and TEM data analysis. Conductive AFM also indicated that the PCBM circumscribed the PS to create a uniform interface.The columnar structure provides large and consistent interfacial areas between the electron donor

and electron acceptor materials, effectively enhancing exciton dissociation efficiency and carrier transportation through the active layer of organic solar cells. Through the confirmation of this uniform columnar structure, the experiment was successful in achieving its goal of creating the ideal OHJ structure, in which conversion efficiency increases because of reduced distance between the electrodes and the active layer.

As hypothesized, the addition of polystyrene resulted in a shorter travel distance through the active layer, reducing the risk of recombination between the electron and its hole. The columnar structure optimized the path of the electron-hole pair, leading to greater efficiency. Furthermore, the addition of graphene to the organic photovoltaic active layer solutions as an additive to facilitate exciton dissociation and carrier transportation was shown to be effective. Collectively, devices containing ideal concentrations of polystyrene and graphene showed increases in short circuit current (J_{SC}) and open circuit voltage (V_{OC}), thus resulting in an increase of 31.72% in energy conversion efficiency (η).

Overall, the device with a ratio of 4:2:12:0.1 (PCDTBT:PS:PCBM:Graphene) resulted in the highest PCE, with an efficiency of 2.525%. This device showed the most ideal ratio of all the organic solar cells, since an increase or decrease of PCBM or graphene resulted in lower efficiencies. Compared to the control device, this combination of materials led to a significantly better performance across all the parameters. Ultimately, the inverted organic cell structure as well as the addition of polystyrene and graphen all contributed to this high PCE.

However, in the future, further investigation could be done. For instance, the ratio of PCDTBT to graphene could be adjusted to determine the optimal solution. Also, since the addition of graphene in organic solar cells has not been widely researched, it would be useful to perform more experiments regarding the implementation of graphene and its effects. The difficulty of dissolving graphene poses the question of discovering better methods of integrating the polymer into the active layer. Although the solubility of graphene in this experiment was adequate for its application, it would be preferable to find more efficient and effective methods for its dissolution. Furthermore, it was difficult to pick up the presence of PCBM

through Raman spectroscopy; thus, other methods of analysis could be explored in order to detect the effects of PCBM on the morphology of the active layer. Future work extending from this experiment would most likely involve the modification of PCDTBT:PS:PCBM:Graphene ratios in order to determine the exact optimal solution. The addition of other polymers could also be experimented with, such as the presence of P3HT with PCDTBT, both of which are electron donors. Or, the simultaneous addition of PCBM and PMMA, which are both electron acceptors.

Nonetheless, here are limitless applications of organic solars cells, especially as society heads towards a future of more widespread sustainable, renewable energy. Record installations of photovoltaic (PV) cells have occured in the past few years, and the numbers are growing exponentially. Since 2008, more than ten times the amount of PVs have been installed globally[19]. The world is headed toward greater technological prominence, and organic solar cells will be easily integrated into those systems. The addition of solar power is becoming desired by a greater range of products, indicating an increased motive to integrate solar cells in daily life. Due to their thinness, organic solar cells are able to be implemented almost anywhere. Even now, companies have begun to add these cells into windows and other transparent materials. The future of technology and science is predicted to be a symbiotic relationship, in which many products will have combinations of organic solar cells, fuel cells, and batteries[5], resulting in many more technological advances. As organic solar cells become more ubiquitous in daily life, it is likeley that more and more applications of these low-efficiency cells will be discovered and implemented into the technologically advancing world.

References

[1] *BHJ Columnar Structure image*. (2011). http://pubs.rsc.org/en/content/articlelanding/2011/jm/c0jm03026k#!divAbstract [1] Brunisholz, M. (Ed.). (2014). 2014 Snapshots of Global PV Markets.

[2] Etzold, F. (2011). Ultrafast Exciton Dissociation Followed by Nongeminate Charge Recombination in PCDTBT:PCBM Photovoltaic Blends. Journal of the American Chemical Society, 133, 9469-9479. Retrieved July 1, 2015, from http://www.researchgate.net/profile/Nam_Seob_Baek/publication/51109147_Ultrafast_Exciton_Dissociation_Followed_by_Nongeminate_Charge_Recombination_in_PCDTBTPCBM_Photovoltaic_Blends/links/0fcfd504e8d28a9ef5000000.pdf

[3] Fang, L. (2013). Side-Chain Engineering of Isoindigo-Containing Conjugated Polymers Using Polystyrene for High-Performance Bulk Heterojunction Solar Cells. American Chemical Society, 25, 4874–4880-4874–4880. doi:10.1021/cm4024259

[4] *Graphene image*. (2014). http://www.pcworld.com/article/2147304/graphene-is-the-super-substance-that-could-replace-silicon-plastic-and-glass.html

[5] Hoppe, H. (2004). Organic solar cells: An overview. Journal of Materials Research, 19(7), 1924-1945. Retrieved July 1, 2015, from http://www.instruction.greenriver.edu/csolomon/Physics/SPRING 2013/Sacricifti reviewl Overview Saricifti 2004.pdf

[6] Kim, J. (2014). Synthesis of PCDTBT-Based Fluorinated Polymers for High Open-Circuit Voltage in Organic Photovoltaics: Towards an Understanding of Relationships between Polymer Energy Levels Engineering and Ideal Morphology Control. American Chemical Society, 6(10), 7523–7534-7523–7534. doi:10.1021/am500891z

[7] Konios, D., Stylianakis, M., Stratakis, E., & Kymakis, E. (2014). Dispersion behaviour of graphene oxide and reduced graphene oxide. Journal of Colloid and Interface Science, 430, 108-112. doi:10.1016/j.jcis.2014.05.033

[8] Li, G. (2005). Investigation of annealing effects and film thickness dependence of polymer solar cells based on poly„3-hexylthiophene…. Journal of Applied Physics, 98. Retrieved July 1, 2015, from http://yylab.seas.ucla.edu/papers/0021-8979_98_043704_2005.pdf

[9] Lim, F. (2012). Influence of a novel fluorosurfactant modified PEDOT:PSS hole transport layer on the performance of inverted organic solar cells. Journals of Materials Chemistry, 22, 25057-25064. doi:10.1039/C2JM35646E

[10] Liu, Z. (2008). Organic Photovoltaic Devices Based on a Novel Acceptor Material: Graphene. Advanced Materials, 3924-3930.

[11] Louwet, F., Groenendaal, L., Dhaen, J., Manca, J., Luppen, J., Verdonck, E., & Leenders, L. (2003). PEDOT/PSS: Synthesis, characterization, properties and applications. Synthetic Metals, 135-136, 115-117. doi:10.1016/S0379-6779(02)00518-0

[12] Maul, J. (2007). Polystyrene and Styrene Copolymers. Ullmann's Encyclopedia of Industrial Chemistry. doi:10.1002/14356007.a21_615.pub2

[13] Movla, H. (2013). Influence of Active Region Thickness on the Performance of Bulk Heterojunction Solar Cells: Electrical modeling and simulation. Re-

trieved July 1, 2015, from http://www.researchgate.net/profile/Hossein_Movla/publication/258832261_Influence_of_Active_Region_Thickness_on_the_Performance_of_Organic_Bulk_Heterojunction_Solar_Cells/links/00b7d52921f9ce2b9a000000.pdf

[14] Pan, C., Li, H., Akgun, B., Satijia, S., Zhu, Y., Xu, D., . . . Rafailovich, M. (2013). Enhancing the Efficiency of Bulk Heterojunction Solar Cells via Templated Self-Assembly. Macromolecules, 46(5), 1812-1819. doi:10.1021/ma302458d

[15] *PCBM image*. (2013). http://pubs.rsc.org/en/content/articlehtml/2013/ee/c3ee41096j

[16] *PCDTBT image*. (2013). http://pubs.rsc.org/en/content/articlehtml/2013/ee/c3ee41096j

[17] *Polystyrene image*. (2008). https://upload.wikimedia.org/wikipedia/commons/thumb/6/60/Polystyrene.svg/150px-Polystyrene.svg.png

[18] Synooka, O. (2014). Modification of the Active Layer/PEDOT:PSS Interface by Solvent Additives Resulting in Improvement of the Performance of Organic Solar Cells. American Chemical Society, 6, 11068−11081-11068−11081. Retrieved July 1, 2015, from http://pubs.acs.org.proxy.library.stonybrook.edu/doi/pdf/10.1021/am503284b

[19] U.S. Solar Market Insight. (2015). Retrieved July 1, 2015, from http://www.seia.org/research-resources/us-solar-market-insight

[20] Wakim, S. (2009). Highly efficient organic solar cells based on a poly(2,7-carbazole) derivative. Journal of Materials Chemistry, 19, 5351-5358. Retrieved July 1, 2015, from http://pubs.rsc.org.proxy.library.stonybrook.edu/en/content/articlepdf/2009/jm/b901302d

[21] Wang, T. (2012). Correlating Structure with Function in Thermally Annealed PCDTBT:PC 70 BM Photovoltaic Blends. Advanced Functional Materials, 22. doi:10.1002/adfm.201102510

[22] Xue, H., Kong, X., Liu, Z., Liu, C., Zhou, J., Chen, W., . . . Xu, Q. (2007). TiO2 based metal-semiconductor-metal ultraviolet photodetectors. Appl. Phys. Lett. Applied Physics Letters, 90(20), 201118-201118. doi:10.1063/1.2741128